Comparative Study Between Two Different Active Flutter Suppression Systems

E. Nissim*
Technion – Israel Institute of Technology, Haifa, Israel

An activated leading-edge (LE) – trailing-edge (TE) control system is applied to a drone aircraft with the objective of enabling the drone to fly subsonically at dynamic pressures which are 44% above the open-loop flutter dynamic pressure. The control synthesis approach is based on the aerodynamic energy concept and it incorporates recent developments in this area. A comparison is made between the performance of the activated LE-TE control system and the performance of a TE control system, analyzed in a previous work. The results obtained indicate that although all the control systems achieve the flutter suppression objectives, the TE control system appears to be somewhat superior to the LE-TE control system, in this specific application. This superiority is manifested through reduced values of control surface activity over a wide range of flight conditions.

Introduction

THE aerodynamic energy approach to problems of flutter suppression using active controls, was developed[1] with the objective of deriving control laws which can stabilize any fluttering aerodynamic system. The results obtained in Ref. 1 indicated the superiority of the combined leading-edge (LE) – trailing-edge (TE) control system over the TE alone or the LE alone control systems within the limits of the assumptions made. Application of the general results of Ref. 1 to specific aircraft[2,3] has demonstrated the effectiveness of the activated LE-TE control system in the simultaneous solution of both flutter suppression and gust alleviation problems. There has been considerable reluctance however to incorporate an activated LE control due to the large hinge moment required to control its motion and due to its possible detrimental effects on the general aerodynamic characteristics of the wing. Recent developments in the aerodynamic energy approach[4] permit the employment of a TE-only control system for the suppression of flutter. Application of these new developments to a specific flutter problem of a drone aircraft[5] has demonstrated the ability of the TE control system to act on its own as a flutter suppressor. A comparison has recently been made[6] between the performance of the activated TE control system, when designed by the application of the relaxed energy approach[4,5] and the performance of a similar control system, when designed by classical control theory. This comparison demonstrated both the effectiveness and the superiority of the control system designed by the aerodynamic energy method.

In the present work, a combined LE-TE control system is applied to the same drone aircraft discussed in Refs. 5 and 6 with the object of comparing the effectiveness of the LE-TE control system with the TE alone control system. The synthesis technique used in the present work is identical to the one developed in Ref. 5 and the general types of control law transfer functions employed herein are identical to the ones developed in Ref. 4.

Description of Flutter Example and of Mathematical Model

Description of the Drone Aircraft

The activated LE-TE control system is applied to a violent wing flutter case of a drone aircraft (Firebee II-BQM-34F) selected by NASA for flight research programs aimed at validating active control system concepts. Figure 1 shows three views of the drone aircraft together with some general aerodynamic data. A single activated LE-TE strip, with a width equal to 12% of the wing semispan and 20% chord control surfaces, is assumed on each wing (see Fig. 2). The strip is located as near the tip as structurally possible in accordance with the results reported in Ref. 3.

Equations of Motion

Let the n equations

$$([B]s^2+\pi b^2 l_s \rho V^2[A]+[E])\{\bar{q}\}=0 \tag{1}$$

represent the equations of motion of n structural modes with r activated control surfaces, where

$$s=i\omega$$

and where ω represents the frequency of oscillation $[B]$ the mass matrix, $[A]$ the complex aerodynamic matrix, $[E]$ the stiffness matrix, ρ the density of the surrounding fluid, V the velocity of the fluid, $2b$ the reference chord, l_s the wing semispan, and $\{\bar{q}\}$ the response vector. All the matrices in Eq. (1) are of order $n\times(n+r)$ (n structural modes $+r$ active controls). The response vector $\{\bar{q}\}$ can be expressed in terms of n structural responses and r control deflections, that is,

$$\{\bar{q}\}=\begin{Bmatrix} q \\ q_c \end{Bmatrix} \tag{2}$$

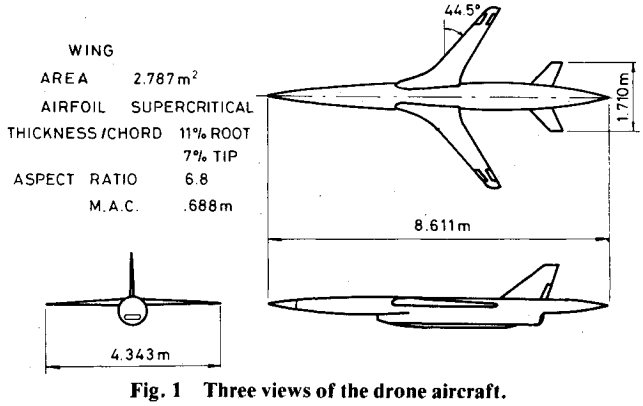

Fig. 1 Three views of the drone aircraft.

Received Jan. 9, 1978; revision received June 7, 1978.

Index category: Aeroelasticity.

*Professor, Dept. of Aeronautical Engineering. Member AIAA.

Equation (1) can therefore be written as

$$([B_s|B_c]s^2+\pi b^2 l_s \rho V^2[A_s|A_c]+[E_s|E_c])\begin{Bmatrix} q \\ q_c \end{Bmatrix}=0 \quad (3)$$

Assume now a control law of the form

$$\{q_c\}=[T]\{q\} \quad (4)$$

where $[T]$ is an $r\times n$ matrix representing the transfer functions of the control law. Substitution of Eq. (4) into Eq. (3) yields

$$\left[([B_s]+[B_c][T])s^2+2\pi b^2 l_s\frac{\rho V^2}{2}([A_s]+[A_c][T])+([E_s]+[E_c][T])\right]\{q\}=0 \quad (5)$$

In general, the elements of the aerodynamic matrices A_s and A_c are functions of the reduced frequency k and the Mach number M, whereas the transfer function matrix $[T]$ is a function of s, expressed in terms of rational polynomials in s. Let the matrix $[T]$ be expressed by

$$[T]=[1/Q(s)][T_N] \quad (6)$$

where $Q(s)$ is a scalar polynomial in s representing the common denominator of all the T_{ij} terms and where $[T_N]$ is a matrix (a function of s) involving the resulting numerators.

The variation with k of the aerodynamic matrix $[A_s|A_c]$ can be approximated by the following representation[7]

$$[A]=[A_0]+[A_1]\left(\frac{b}{V}\right)s+[A_2]\left(\frac{b}{V}\right)^2 s^2+\sum_{j=1}^{4}\frac{[D_j]s}{s+(V/b)\gamma_j} \quad (7)$$

where all the matrix coefficients and the γ_j's are constants.

Substitution of Eqs. (6) and (7) into Eq. (5) and multiplication of the resulting equation by $Q(s)$ yields a matrix polynomial expression with s of the form

$$[F_0]+[F_1]s+[F_2]s^2+\ldots+[F_m]s^m)\{q\}=0 \quad (8)$$

where the matrix coefficients $[F_j]$ are functions of M, V, and $\frac{1}{2}\rho V^2$. Equation (8) can be reduced to the following canonical form for eigenvalue solution

$$s\{X\}=[U]\{X\} \quad (9)$$

where $[U]$ is of order $(m\times n)\times(m\times n)$ defined by

$$[U]=\begin{bmatrix} [-F_m^{-1}F_{m-1}] & [-F_m^{-1}F_{m-2}] & \ldots & [-F_m^{-1}F_0] \\ [I] & 0 & \ldots & 0 \\ 0 & [I] & \ldots & 0 \\ \vdots & & & \\ 0 & 0 & [I] & 0 \end{bmatrix} \quad (10)$$

and $\{X\}$ is given by

$$\{X\}=\begin{Bmatrix} s^{m-1}\{q\} \\ s^{m-2}\{q\} \\ \vdots \\ s\{q\} \\ \{q\} \end{Bmatrix} \quad (11)$$

Solution for Flutter

Since the velocity of sound varies only slightly with altitude, the value of V follows the choice of the value of Mach number M. The matrix $[U]$ will, therefore, depend only on $Q_D\,(=\frac{1}{2}\rho V^2)$ for any given value of M. Any variations in Q_D should therefore be regarded as resulting from changes in altitude while keeping M constant. Equation (9) is solved for a chosen value of $[T]$ over a range of values of Q_D and the results presented by root locus type plots taking Q_D as a parameter.

Mathematical Model

In the present example, nine symmetric structural modes are considered (that is, two rigid-body modes + seven elastic modes). The generalized matrices $[B]$, $[E]$ and the natural mode shapes are determined using a finite-element Nastran model consisting of 127 modes. The generalized aerodynamic matrices $[A]$ and the generalized gust force (per unit gust velocity) $\{F_G\}$ are computed for different values of Mach number and reduced frequencies by using the Doublet Lattice method with 135 boxes.

Control Laws

The general form of the control laws employed in this work was established in Ref. 4. The application of these control laws to the current flutter example is identical to the one described in Ref. 5. In general, the control laws are given by

$$\begin{Bmatrix} \beta \\ \\ \delta \end{Bmatrix}=[\bar{T}]\begin{Bmatrix} \dfrac{h_l-h_r}{b} \\ \\ \alpha-\alpha_r \end{Bmatrix} \quad (12)$$

where β and δ are the deflections of the LE and TE control surfaces, respectively (Fig. 2), and where h_l, h_r, α, α_r, and b are measured at the locations indicated in Fig. 2.

The response vector in Eq. (12) can be expressed in terms of the n natural mode shapes through the use of the modal matrix $[H]$, that is,

$$\begin{Bmatrix} \dfrac{h_l-h_r}{b} \\ \\ \alpha-\alpha_r \end{Bmatrix}=[H]\{q\} \quad (13)$$

Equation (12) can therefore be written as

$$\begin{Bmatrix} \beta \\ \delta \end{Bmatrix}=[\bar{T}][H]\{q\} \quad (14)$$

Therefore,

$$[T]=[\bar{T}][H] \quad (15)$$

The control law is expressed in terms of the relative response vector following the results presented in Ref. 3 which demonstrated the advantages in considering only the relative elastic deformation while "filtering" out the rigid-body responses from the input of the control law. The transfer function matrix $[\bar{T}]$ is of order 2×2. Two general types of $[\bar{T}]$ will be considered, in conformity with the results of Ref. 4 and their application in Ref. 5. The first type of $[\bar{T}]$, referred to as the localized damping type transfer function (LDTTF) is given by

$$[\bar{T}]=\begin{bmatrix} 0 & 0 \\ 0 & -1.86 \end{bmatrix}+\begin{bmatrix} R_L & 0 \\ 0 & R_T \end{bmatrix}\begin{bmatrix} -4 & 4 \\ 4 & 2.8 \end{bmatrix} \quad (16)$$

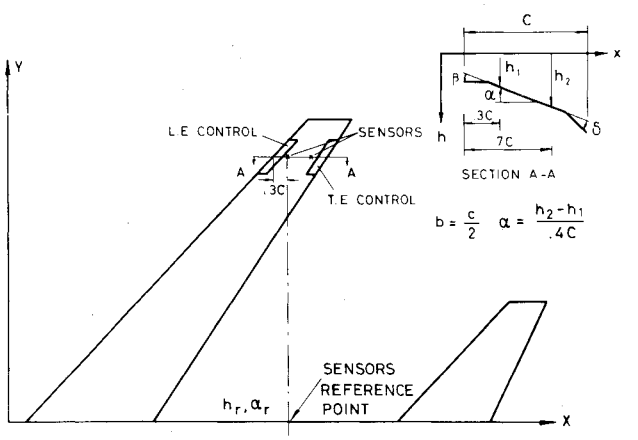

Fig. 2 Geometrical description of the active control system.

where R_L and R_T are given by

$$R_L = \frac{a_{L1}s^2}{s^2+2\zeta_{L1}\omega_{n_{L1}}s+\omega^2_{n_{L1}}} + \frac{a_{L2}s^2}{s^2+2\zeta_{L2}\omega_{n_{L2}}s+\omega^2_{n_{L2}}} \quad (17)$$

$$R_T = \frac{a_{T1}s^2}{s^2+2\zeta_{T1}\omega_{n_{T1}}s+\omega^2_{n_{T1}}} + \frac{a_{T1}s^2}{s^2+2\zeta_{T2}\omega_{n_{T2}}s+\omega^2_{n_{T2}}} \quad (18)$$

The parameters a_{Lj}, a_{Tj}, ζ_{Lj}, ζ_{Tj}, $\omega_{n_{Lj}}$, and $\omega_{n_{Tj}}$ are all positive and their values determined by an optimization program based on the gust response of the aircraft under consideration, following the method of Ref. 5. Description of the optimization procedure is presented in the following section so as to maintain some measure of self-containment of the present work. It is shown in Ref. 4 that a_{Lj} and a_{Tj} control the amount of aerodynamic damping introduced by the control surface, ω_{nL} and ω_{nT} determine the frequencies around which the largest values of damping are introduced, and ζ_L and ζ_T control the distribution of damping at frequencies around the respective ω_{nL} and ω_{nT}. The second type of $[\bar{T}]$, referred to as the damping type transfer function (DTTF), is given by

$$[\bar{T}] = \begin{bmatrix} 0 & 0 \\ 0 & -1.86 \end{bmatrix} + \frac{s}{\omega_R}\begin{bmatrix} a_L & 0 \\ 0 & a_T \end{bmatrix}\begin{bmatrix} -4 & 4 \\ 4 & 3.2 \end{bmatrix} \quad (19)$$

where a_L and a_T are positive free parameters which control the amount of aerodynamic damping introduced by the control surfaces and are determined in a similar fashion as in the case of the LDTTF and where ω_R is a reference frequency which maintains the nondimensional nature of a_L and a_T (ω_R is normally assigned the value of the open-loop flutter frequency).

Optimization Procedure – Basic Concept

An optimization procedure which sets out to find the values of control parameters that maximize the flutter dynamic pressure may ultimately lead to an impractical solution due to the resulting excessive control surface activity in a turbulent atmosphere. A more rational approach is to select a range of dynamic pressures within which stability is required and determine the values of the control parameters which yield the desired stability with minimum control surface activity (that is, minimum control surface rates or deflections). Hence, the objective of the optimization procedure to be described in the present work will be to define a design which leads to stability with minimum control surface activity rather than a design which leads to maximum flutter dynamic pressure. To accomplish such a design, the free parameters in either the LDTTF's or DTTF's are assigned initial values that stabilize the system above the required flutter velocity margin. The final values of the free parameters are determined by minimizing the response of the control surface to a gust input. This minimization maintains the stability of the system since any substantial deterioration in stability is accompanied by an increase in the response of the system to gust inputs and hence, by virtue of the assumed control laws [see Eq. (4)], the activity of the control surface must also increase.

Definition of the Target Function

The results of Ref. 5 have indicated that the control surface rates are more critical than the control surface deflections from the point of view of design. Therefore, the target function for minimization using the optimization procedure developed in Ref. 5 is formulated in terms of control surface rates. The control rate activity is therefore defined as the rms control rates per unit rms gust input, based on the Von Kármán gust spectrum.[8] In the case of the TE control system,[5] the target function for minimization was defined as the rms activity of the TE control. In the case of the LE-TE control system employed in the present work, the target function is defined as the sum of the rms activities of the two control surfaces.

Optimization Steps

The basic steps required for optimization are:

1) Select a control law type (LDTTF or DTTF) and assign initial values to the free parameters that stabilize the aeroelastic system at the desired flight velocity and Mach number.

2) Calculate the rms control surface activity per unit rms gust input for the control law by using a continuous gust response analysis.

3) Determine the values of the free parameters which result in minimum control activity.

Selection of the initial values of the free parameters is not as arbitrary as it may appear. Further details regarding this point are presented in Ref. 5.

As can be seen, the optimized control law is determined solely on the basis of gust response analysis rather than on flutter considerations. The implications of this process are: 1) a more rational control design as already discussed in previous sections of this work; 2) reduced computational time, since there is no need to solve large eigenvalue problems associated with the flutter calculations; and 3) simplicity, since it is not necessary to follow discrete eigenvalue branches associated with each response mode.

Flutter Suppression Objectives

The following objectives were set for achievement by the activated drone aircraft. (These objectives are identical to those of Ref. 5.)

1) The drone should be able to fly at $M=0.9$ with a value of Q_D which is 44% above the open-loop flutter dynamic pressure (denoted as $Q_{D_{\max}}$) and with minimum control activity.

2) The stability of the system should be maintained using fixed control gains with no substantial degradation in control activities for all values of $M \leq 0.9$ and $Q_D \leq Q_{D_{\max}}$.

Representation and Discussion of Results

The effectiveness of the activated LE-TE control system can only be assessed by comparison with the open-loop system and the activated TE only system presented in Ref. 5. Therefore, in order to maintain some measure of self-containment of the present work, a very short presentation of the essential results of Ref. 5 will be given here. The open-loop root locus plot at $M=0.9$ is presented in Fig. 3 as an example of the open-loop behavior of the system considered herein (yielding the value of Q_D at flutter: $Q_{DF}=24.07$ kPa). The values of Q_{DF} at the other Mach numbers together with the behavior of the optimum TE control system are presented

Table 1 Summary of numerical results

	Open-loop flutter	Activated system using LDTTF		Activated system using DTTF	
		LE-TE	TE only[a,b]	LE-TE	TE only[a]
Flutter Q_D in kPa:					
$M=0.9$	24.07	54.1	42.49	51.71	43.67
$M=0.7$	27.77	> 59.85	50.03	59.85	51.23
$M=0.5$	29.69	> 59.85	58.41	> 59.85	> 59.85
Max $(\dot{\beta}_{rms}+\dot{\delta}_{rms})$, deg/s/m/s[c]:					
$M=0.9$	...	262.7	253.2	250.7	241.1
$M=0.7$	...	284.5	250.6	257.6	239.1
$M=0.5$[d]	...	128.6	200.1	176.5	183.4
Max $(\beta_{rms}+\delta_{rms})$, deg/m/s[c]:					
$M=0.9$	...	2.95	3.80	2.85	3.80
$M=0.7$	...	2.85	3.15	2.56	3.12
$M=0.5$[d]	...	1.41	1.97	1.57	1.87

[a] Results from Ref. 5.
[b] Relates to the case where $\omega_{n_{T1}}$ and $\omega_{n_{T2}}$ are restricted within the range of $60 \le \omega_{n_{T1}}, \omega_{n_{T2}} \le 150$.
[c] Results of $Q_D \le Q_{D_{max}}$.
[d] Q_D limited up to sea level values (17.69 kPa).

alongside the results of the present work in the summarizing Table 1.

Results for Control Law Based on the LDTTF

The results obtained for the LE-TE control system were very surprising in that they yielded optimum gains which degenerated the system into a TE control system (that is $a_{L1}=a_{L2}=0$) with $\beta=\dot{\beta}=0$. In order to obtain results for the LE-TE control system, constraints were introduced so as to minimize the control activity with $\dot{\beta}_{rms}=\dot{\delta}_{rms}$. The optimization procedure yields the following optimal control law (for $M=0.9$):

$$\beta=\frac{0.92\,s^2}{2^2+2\times0.49\times125s+(125)^2}\lfloor -4 \quad 4\rfloor [H]\{q\}$$

$$\delta=\left[\lfloor 0 \quad -186\rfloor+\frac{0.47\,s^2}{s^2+2\times0.36\times25s+(25)^2}\right.$$

$$\left.+\frac{1.1\,s^2}{s^2+2\times1\times112s+(112)^2}\times\lfloor 4 \quad 2.8\rfloor\right]\lfloor H\rfloor\{q\} \qquad (20)$$

with

$$\dot{\beta}_{rms}=\dot{\delta}_{rms}=131.33 \text{ deg/s/m/s}$$

$$\beta_{rms}=1.08 \text{ deg/m/s}$$

$$\delta_{rms}=1.87 \text{ deg/m/s}$$

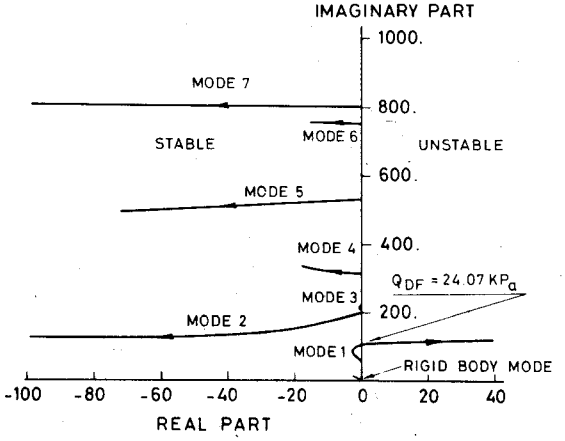

Fig. 3 Open-loop root locus plot at $M=0.9$ (no controls).

yielding the following total activity:

$$\dot{\beta}_{rms}+\dot{\delta}_{rms}\sim 2.62.7 \text{ deg/s/m/s (minimized by the optimization program)}$$

$$\beta_{rms}+\delta_{rms}=2.95 \text{ deg/m/s}$$

The meaning of the different parameters in the control law [Eq. (20)] is explained in both Refs. 4 and 5.

The foregoing results show that for minimum control rates (with $\dot{\beta}_{rms}=\dot{\delta}_{rms}$), damping is introduced around the frequencies of 112-125 rad/s by both the LE and the TE control surfaces. This latter distribution in damping is fairly wide, as implied by $\zeta_{L,1}=0.49$ and $\zeta_{T,2}=1$. At the low-frequency range however, damping is introduced by the TE control surface only, around $\omega=25$ rad/s, with a fairly peaky type of distribution, as implied by $\zeta_{T,1}=0.36$. The first rational transfer function in Eq. (20) which relates to the TE control surface, introduces positive aerodynamic stiffness terms at frequencies larger than 25 rad/s, whereas the remaining rational terms in Eq. (20) introduce positive aerodynamic stiffness terms at frequencies larger than about 112-125 rad/s.

The PSD's (Power Spectral Densities) of the control surface rates are shown in Fig. 4. As can be seen, the rates $\dot{\beta}_{PSD}$, $\dot{\delta}_{PSD}$ show a peak around 20 Hz, that is, around 125 rad/s which is in the vicinity of the open-loop flutter frequency.

An example of a root locus plot for the activated LE-TE control system with the control law given by Eq. (20) is shown in Fig. 5 for $M=0.9$. It can be seen that $Q_{DF}=54.1$ kPa for $M=0.9$ whereas for $M=0.7$ and $M=0.5$ (root locus plots not shown) this same control law yields Q_{DF} values larger than 59.85 kPa (beyond the range of variation of Q_{DF}).

Investigation of the variation of the rms control activity with Q_D (for $Q_D \le Q_{D_{max}}$) using the control law given by Eq. (20) has shown that, for each Mach number, the control activity reduces monotonically with Q_D. The maximum control activity for both the LE and TE control surfaces at different Mach numbers is summarized in Table 1. As can be noted, there is a slight increase in the control rate activity at $M=0.7$. Such small increases in control activity may occur since it is a result of a balance between many factors which affect the system.

Results for Control Law Based on the DTTF

Here again, the results obtained for the LE-TE control system yield optimum gains which degenerate the system into a TE control system (that is $a_L=0$). In order to obtain results

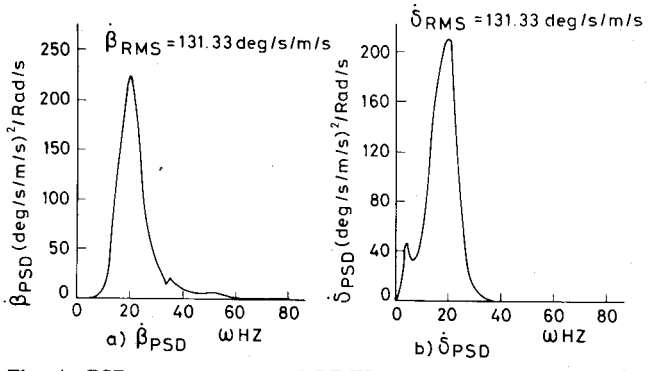

Fig. 4 PSD response rates of LE-TE control surfaces at $M=0.9$ using LDTTF.

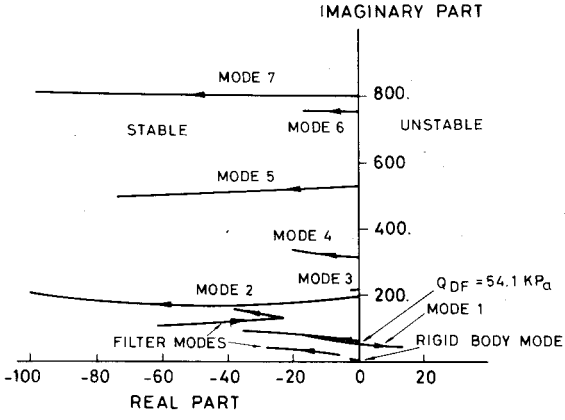

Fig. 5 Closed-loop root locus plot at $M=0.9$ for LE-TE control system using LDTTF.

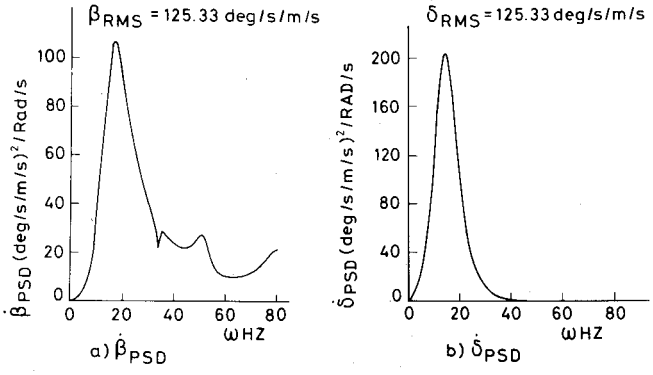

Fig. 6 PSD response rates of LE-TE control surfaces at $M=0.9$ using DTTF.

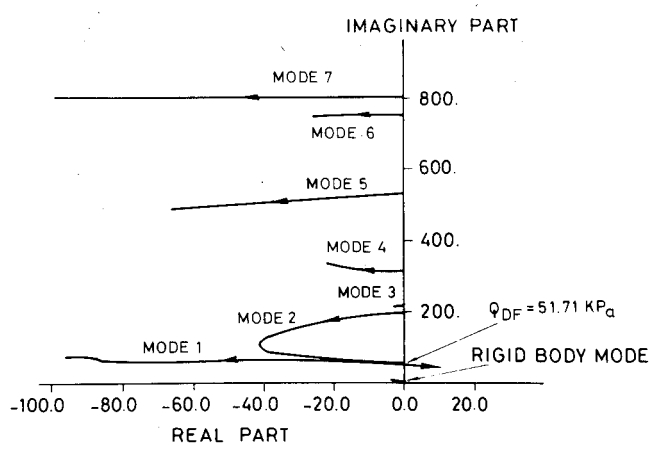

Fig. 7 Closed-loop root locus plot at $M=0.9$ for LE-TE control system using DTTF.

for the LE-TE control system constraints were introduced, similar to the LDTTF case, which minimize the control rate activity with $\dot{\beta}_{rms}=\dot{\delta}_{rms}$. The optimization procedure, with the above constraints, yields the following optimal control law (for $M=0.9$):

$$\beta = 0.75\frac{s}{100}\lfloor -4 \quad 4\rfloor [H]\{q\}$$

$$\delta = \left[\lfloor 0 - 1.86\rfloor + 1.48\frac{s}{100}\lfloor 4 \quad 3.2\rfloor\right][H]\{q\} \qquad (21)$$

with

$$\dot{\beta}_{rms}=\dot{\delta}_{rms}=125.33 \text{ deg/s/m/s}$$

$$\beta_{rms}=1.08 \text{ deg/m/s}$$

$$\delta_{rms}=1.77 \text{ deg/m/s}$$

with the following total activity:

$$\dot{\beta}_{rms}+\dot{\delta}_{rms}=250.7 \text{ deg/s/m/s (minimized by the optimization program)}$$

$$\beta_{rms}+\delta_{rms}=2.85 \text{ deg/m/s}$$

The PSD's of the control surface rates are shown in Fig. 6. Here again the rates $\dot{\beta}_{PSD}$, $\dot{\delta}_{PSD}$ show a peak around the flutter frequency. It should be noted that the PSD curve for the LE control rate does not reduce to a zero level at the high-frequency range. This indicates that the value of β_{rms} should be somewhat higher than the one quoted above.

An example of a root locus plot for the activated LE-TE control system with the control law given by Eq. (21) is shown in Fig. 7 for $M=0.9$. It can be seen that $Q_{DF}=51.71$ kPa for $M=0.9$ whereas for $M=0.7$ and $M=0.5$ (root locus plots not shown) this same control law yields Q_{DF} values larger than 59.85 kPa (beyond the range of variation of Q_{DF}).

Investigation of the variation of the rms control rate activity with Q_D (for $Q_D \le Q_{D_{max}}$), using the control law given by Eq. (21) has shown that, for each Mach number, the control activity reduces monotonically with Q_D. The maximum control activity for the LE-TE control system at different Mach numbers is summarized in Table 1. Here again, a slight increase in the control rate activity at $M=0.7$ can be observed.

Discussion of Results

Table 1 summarizes the results of the present investigation for both the LDTTF and the DTTF. In addition, results pertaining to the optimum TE control system, as obtained from Ref. 5, are presented (in Table 1) for comparison.

It can be seen that the flutter suppression objectives, as stated earlier in this work, have been achieved by all the systems considered (that is, TE alone and LE-TE control system). This is true since the dynamic pressure at flutter, of the activated systems are in all cases larger than $Q_{D_{max}}$ (=34.62 kPa) and since there is no significant degradation in control activity with changes in either Q_D (for $Q_D \le Q_{D_{max}}$) or M. The different control systems should therefore be compared on the basis of their activated control activity rather than their increase in flutter dynamic pressure. The superiority of the TE control system as compared with the LE-TE control system for the specific example treated herein is therefore a direct result of the definition of the target function. Although the definition of the target function for the TE control system is self-evident, its definition for the LE-

TE control system needs some explanation. The LE-TE system consists of two control surfaces, whereas the TE system consists of a single control surface. It can therefore be argued that if an additional TE control surface is added to the TE system (instead of adding an LE control) a reduction in the activity of each of the TE control surfaces can be achieved. It is also reasonable to expect that the activity of the TE control surface is inversely proportional to its span. Hence, by adding a second TE control surface (keeping the spans of both control surfaces equal), the activity of each of the TE control surfaces is expected to be reduced to half its value. However, the sum of the activities of these two TE control surfaces will be equal to the activity of the single TE control surface. The comparison between the TE control system and the LE-TE control system, based on the sum of the activities of the control surfaces in each system, is therefore equivalent to the comparison between a TE-TE control system (with equal spans) and an LE-TE control system. Clearly, only such a comparison can reveal whether the addition of an LE control is superior to the addition of a second TE control to the activated system. It is therefore extremely interesting to note that from the point of view of control surface activity, the TE control system is superior to the LE-TE system for the specific example considered herein. On the other hand, the LE-TE system yields higher flutter speeds than those of the TE control system ($Q_{DF} \sim 52$ kPa for the LE-TE system as compared with $Q_{DF} \sim 43$ kPa for the TE system at $M = 0.9$). These values of Q_{DF} are much higher than those of $Q_{D_{max}}$ and therefore have no direct practical advantage for design. It appears therefore, that although the LE-TE system is more effective (than the TE system) in introducing aerodynamic damping forces into the system, this accomplishment is achieved in the present application at the expense of a slight increase in control surface activity (which is a disadvantage for practical designs). This latter increase in control surface activity is a consequence of the relationship between the stabilizing control surface aerodynamic forces and the response of the system which is dependent on the inertia and elastic characteristics of the structural modes at flutter. Therefore, it is stressed that this result is of a specific nature and should not be generalized to other flutter suppression systems.

Comparison between the results for the LE-TE control system using the two different types of transfer functions shows a slight superiority of the DTTF over the LDTTF. This slight superiority is, however, overshadowed by the fact that the rms activity of the LE control has not reached a converged value (see Fig. 6) and the possibility of instability at high frequencies.[4]

It may be noted that the DTTF requires the optimization of only two variables for the LE-TE control system, as compared with twelve variables required by the LDTTF while control activities have very similar values. This fact can be used for preliminary design work when a small number of variables is of considerable advantage. The LDTTF can then be used for purposes of achieving a more refined and more practical design.

Conclusions

Application of an activated LE-TE control surface to a drone aircraft for purposes of flutter suppression yields somewhat inferior results to those of a TE control system. Although this finding is of a specific nature and does not necessarily hold true for other applications it is of great importance since it shows that a TE control system (as derived through the application of the relaxed aerodynamic energy approach) can yield results which compare favorably with an LE-TE control system.

Acknowledgments

This work is part of a study supported by NASA under Grant NSG-7072.

References

[1] Nissim, E., "Flutter Suppression Using Active Controls Based on the Concept of Aerodynamic Energy," NASA TN D-6199, 1971.

[2] Nissim, E., "Flutter Suppression and Gust Alleviation Using Active Controls," NASA-CR 138658 (also TAE Rept. 198), 1974.

[3] Nissim, E., Caspi, A., and Lottati, I., "Application of the Aerodynamic Energy Concept to Flutter Suppression and Gust Alleviation by Use of Active Controls," NASA TN D-8212, 1976.

[4] Nissim, E., "Recent Developments in the Aerodynamic Energy Concept," NASA TN D-8519, 1977 (presented in part at the 18th AIAA Structural Dynamics and Dynamics Conference, March 1977).

[5] Nissim, E. and Abel, I., "Development and Application of an Optimization Procedure for Flutter Suppression Using the Aerodynamic Energy Concept," NASA Tech. Paper 1137, Feb. 1978.

[6] Abel, I., Perry, B. III, and H.N. Murrow, "Synthesis of Active Controls for Flutter Suppression on a Flight Research Wing," AIAA Paper 77-1062, AIAA Guidance and Control Conference, Aug. 1977.

[7] Sevart, F.D., "Development of Active Flutter Suppression Wind Tunnel Testing Technology," AFFDL-TR-74-126, 1975.

[8] Pratt, K.G., "Response of Flexible Airplanes to Atmospheric Turbulence," *Performance and Dynamics of Aerospace Vehicles*, NASA SP-258, 1971.